

(*e, 3e*) on Helium at Low Impact Energy: The Strongly Correlated Three-Electron ContinuumM. Dürr,¹ A. Dorn,¹ J. Ullrich,¹ S. P. Cao,² A. Czasch,³ A. S. Kheifets,⁴ J. R. Götz,⁵ and J. S. Briggs⁵¹Max-Planck-Institute for Nuclear Physics, Saupfercheckweg 1, 69117 Heidelberg, Germany²Institute of Modern Physics, Chinese Academy of Science, Graduate University of Chinese Academy of Science, Lanzhou 730000, China³Institut für Kernphysik, Universität Frankfurt, D-60438 Frankfurt, Germany⁴Australian National University, Canberra ACT 0200, Australia⁵University Freiburg, Hermann-Herder-Strasse 3, 79104 Freiburg, Germany

(Received 16 August 2006; published 11 May 2007)

Double ionization of the helium atom by slow electron impact ($E_0 = 106$ eV) is studied in a kinematically complete experiment. Because of a low excess energy $E_{\text{exc}} = 27$ eV above the double ionization threshold, a strongly correlated three-electron continuum is realized. This is demonstrated by measuring and calculating the fully differential cross sections for equal energy sharing of the final-state electrons. While the electron emission is dominated by a strong Coulomb repulsion, also signatures of more complex dynamics of the full four-body system are identified.

DOI: [10.1103/PhysRevLett.98.193201](https://doi.org/10.1103/PhysRevLett.98.193201)

PACS numbers: 34.80.Dp

Small systems of Coulomb interacting particles such as the helium atom or the hydrogen molecule have been models for quantum theory since its earliest days. While nearly exact calculations for such systems are available for static, bound state properties, dynamical reactions have proven to be much more difficult to describe theoretically. It was only recently that the dynamics of fundamental three-body systems such as low-energy electron-impact single ionization of atomic hydrogen [1] or double photoionization of helium [2,3] could be calculated accurately. Problems still persist for particle impact single ionization of more complex targets than hydrogen as observed even for the most simple multielectron target helium [4]. Experimental and theoretical studies of processes leading to the four-body breakup are still in their infancy. Examples for photon-induced reactions are triple ionization of lithium and the complete photofragmentation of the deuterium molecule. For the first reaction, so far only total cross sections could be measured [5]. For the second reaction fully differential cross sections (FDCS) revealed complex structures in the electron emission pattern [6,7]. Some key features of these experiments have been reproduced in a recent *ab initio* calculation [8]. In addition, many selection rules for the double photoionization of molecular hydrogen have been proven [9,10]. However, because the target nuclei can be taken as fixed, during the time required for the electrons to escape the molecule, the photoionization of the hydrogen molecule is a much less challenging problem as compared with electron-impact ionization of the helium atom.

Collisions of charged particles with atoms can lead to the emission of several strongly correlated electrons; e.g., Schulz *et al.* have demonstrated the strong correlation of three electrons emitted in collisions of fast, highly charged ions with neon atoms [11]. The most fundamental four-body process is represented by double ionization of he-

lium. Highly differential experiments for this reaction have been performed for various ion species (see, e.g., [12,13]) and for electrons [14,15]. So far, fully differential studies were restricted to fast electron impact with $E_0 \geq 500$ eV, $v_0 \geq 6$ a.u. In this so-called perturbative regime, the projectile-target interaction is weak and well described by the lowest terms of the Born series. Thus, the reaction can be represented by an effective three-body model involving only the helium fragments. Furthermore, in most collisions the projectile scattering angles and, therefore, the momentum transfers are small, and the cross sections very closely resemble these observed in double photoionization of helium being governed by the dipole selection rules. For these reasons, various few-body Coulomb methods [16,17] or the convergent close coupling (CCC) method in combination with the first [18] or second Born approximation [19] were in good agreement with the experimental data on a relative scale.

The full complexity inherent in the four-body dynamics appears only at lower projectile velocities where all of the mutual two-body forces involved are of the same magnitude. Particularly interesting is the threshold region, where theory predicts that double ionization should proceed via a small subspace of the full many-body configuration space in which the electrons are always at similar distances from the ion and form an equilateral triangle in order to minimize their repulsion [20,21]. This strongly restricted accessible phase space results in a very small cross section. Therefore, closely above the double ionization threshold $IP = 79$ eV only total cross section measurements exist [22], and this low-energy regime is completely unexplored so far as fully differential measurements are concerned.

In this Letter, we present a combined experimental and theoretical study of the FDCS for low-energy ($E_0 = 106$ eV) electron-impact double ionization of helium. In order to perform these measurements of a cross section of

the order of 10^{-20} cm², which is about 5% of the maximum cross section for electron-impact double ionization at $E_0 = 300$ eV, a newly developed advanced reaction microscope was employed. This apparatus opens the way to the detailed study of breakup reactions close to threshold. Since a large part of the complete phase space of the three final-state electrons carrying the excess energy of $E_{\text{exc}} = 27$ eV is covered, detailed insight into the breakup dynamics in the nonperturbative regime is gained.

The multicoincidence multielectron recoil-ion momentum spectrometer is shown schematically in Fig. 1 [23]. A well focused (1 mm), pulsed electron beam (pulse length ≈ 1.5 ns, repetition rate 200 kHz, $\approx 10^4$ electrons/pulse), produced by a standard thermo cathode gun, crosses, and ionizes a supersonic He jet (1 mm diameter, 10^{12} atoms/cm³). Using parallel electric (1 V/cm) and magnetic (6 G) fields, the fragments in the final state are projected onto 2D position- and time-sensitive multihit channel plate detectors equipped with delay-line readout. In this way, a large part of the full solid angle is covered, 100% for the detection of target ions, and 80% for electrons below 15 eV. From the positions of the hits and the time of flight, the vector momenta of the particles can be calculated.

In contrast to previous designs [24], in the present reaction microscope the projectile beam axis (defining the longitudinal direction) is adjusted exactly parallel to the electric and magnetic extraction fields. On the one hand, this arrangement facilitates the guiding of slow projectile beams into the target and scattered projectile electrons with a transverse momentum of $0.2 \leq p_{\perp} \leq 1.2$ a.u. can be detected as well. On the other hand, a central bore (5 mm diameter) in the forward electron detector is required to allow for the passage of the non-deflected electrons. It is also to be noted that, due to the jet velocity transversal to the extraction direction, ions have an offset momentum of $p_{\perp} \approx 6$ a.u., and the ion detector is located off the projectile beam axis.

For the present experiments, as for typical ion-impact data, the recoil-ion momentum resolution [full width at half maximum (FWHM)] is $(\Delta p_{\perp}, \Delta p_{\parallel}) \approx (0.4, 0.15)$ a.u.

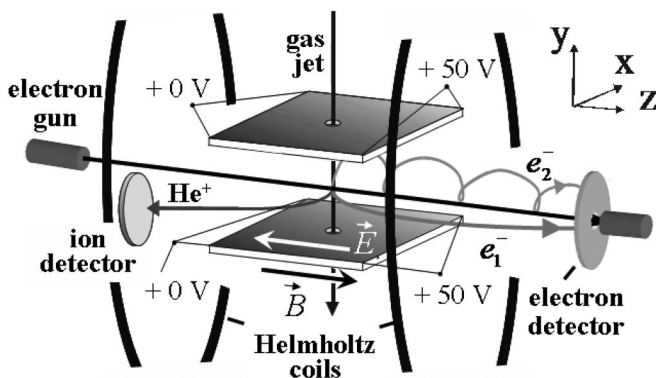


FIG. 1. Scheme of the experimental setup.

For all electrons, including the scattered ones, the transversal resolution is $\Delta p_{\perp} \leq 0.1$ a.u. (FWHM). The longitudinal resolution for the electrons is $\Delta p_{\parallel} \leq 0.02$ a.u. (FWHM).

The normalization of the $(e, 3e)$ cross section has been performed by measuring simultaneously both double and single ionization events within the same experimental run and therefore fixing their relative scale. The resulting $(e, 2e)$ cross sections were normalized to those obtained by Ehrhardt, published in Ref. [25] at identical kinematical parameters (ejected electron energies, angles, momentum transfer, and coplanar geometry) except for the small difference of 6% between the electron-impact energies used in the two experiments (106 eV in the present work and 100 eV in the Ehrhardt experiment). This was corrected for by scaling our data using a three-body double continuum Coulomb wave function (3C) calculation [23]. Thus, a possible additional error due to 6% difference in impact energy is reduced to a negligibly small amount.

In order to demonstrate a strong angular correlation between the three final-state continuum electrons, the cross section is plotted in Fig. 2 as a function of their relative emission angles. While θ_{12} is the angle enclosed by the momentum vectors of two arbitrarily chosen final-state electrons e_1 and e_2 , θ_{23} is the respective angle enclosed by e_2 and the residual electron e_3 . The diagram contains all double ionization events recorded regardless of how the excess energy is shared among the electrons or into which direction the electrons are emitted with respect to the incoming beam. It is clear that the cross section displayed in Fig. 2 reflects a situation far from uncorrelated emission which would have resulted in a uniform and structureless pattern. Electron emission is allowed only along a ridge going from top center to the right center of the diagram

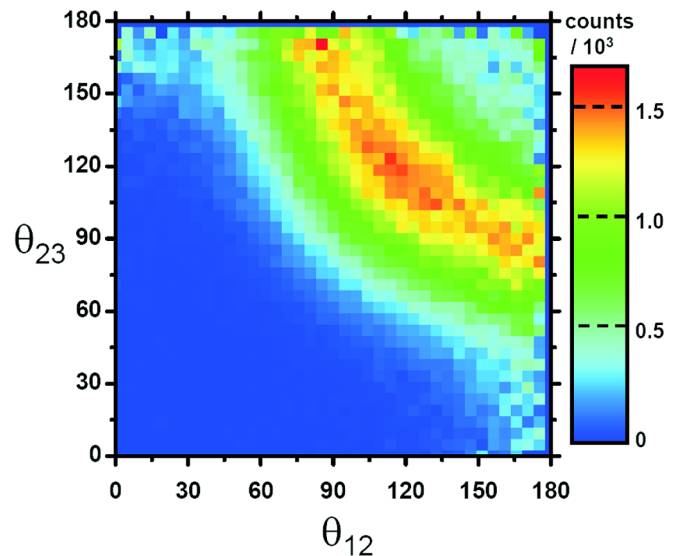


FIG. 2 (color online). Cross section differential in the relative emission angle θ_{12} and θ_{23} .

(corresponding to emission from a back-to-back configuration of two electrons with the third one emitted perpendicular to the others) to a symmetric configuration where the electron trajectories enclose angles of approximately 120° . Small relative angles $\theta_{12}, \theta_{23} < 90^\circ$ are excluded. The top right region in the diagram corresponds to small angles for $\theta_{13} \leq 360^\circ - \theta_{12} - \theta_{23}$ which are suppressed also. Thus, we are in an energy range where the three continuum electrons are strongly correlated. The threshold regime, where, according to theoretical predictions [20,21], only the symmetric emission should be present with relative angles $\theta_{ij} = 120^\circ$, has not yet apparently been reached in the present experiment. It is important to note that the observed configurations with large relative emission angles imply that the electrons' sum momentum is rather small. Indeed, we observe that a large fraction of the projectile momentum $p_0 = 2.8$ a.u. is carried by the residual ion with a high mean longitudinal momentum of $p_R^\parallel \approx 2.4$ a.u. Therefore, there must be either a strong momentum transfer to the ion during the collision or double ionization is selective on the large momentum components in the initial state wave function. In the latter case, theoretical calculations may become very sensitive to the details of the electronic wave function.

In Fig. 3, FDCS are presented for equal energy sharing $E_1 = E_2 = E_3 = 9$ eV and the coplanar scattering geometry where the emitted electrons are ejected in a common plane containing the incoming projectile direction. The cross sections are plotted as a function of one electron emission angle θ_3 with respect to the incoming beam forward direction for a fixed emission angle $\theta_1 = 45^\circ$ and three different angles $\theta_2 = 135^\circ$ (a), 225° (b), and 315° (c). Consistent with the cross section pattern in Fig. 2 discussed above, the electron-electron repulsion also dominates emission in the coplanar kinematics with equal energy sharing. For emission angles θ_3 in the vicinity of θ_1 and θ_2 , the cross section is vanishing. Furthermore, as can be seen in Figs. 3(a) and 3(c) for an angular separation $|\theta_2 - \theta_1| = 90^\circ$, emission of the third electron in between e_1 and e_2 is suppressed (i.e., in the vicinity of 90° and 0° , respectively), and only one broad peak in the cross section is observed. For the back-to-back emission $|\theta_2 - \theta_1| = 180^\circ$, two relatively narrow maxima with angles around 90° with respect to the fixed electrons direction show up.

Theoretically, emission characteristics of low-energy ($E_{\text{exc}} = 6$ eV) electron-impact double ionization was first studied using a six Coulomb wave function approach (6C) which took into account the interactions of all six two-body subsystems present within the four-particle system [21]. Results of this study indicated the presence of the maxima at the mutual angle values $\theta_{12} = 180^\circ$, $\theta_{23} = 90^\circ$ and $\theta_{12} = 120^\circ$, $\theta_{23} = 120^\circ$, which is consistent with the cross section pattern displayed in Fig. 2. To describe the results of the present study, we employ an improved DS6C final-state wave function which is the dynamically screened

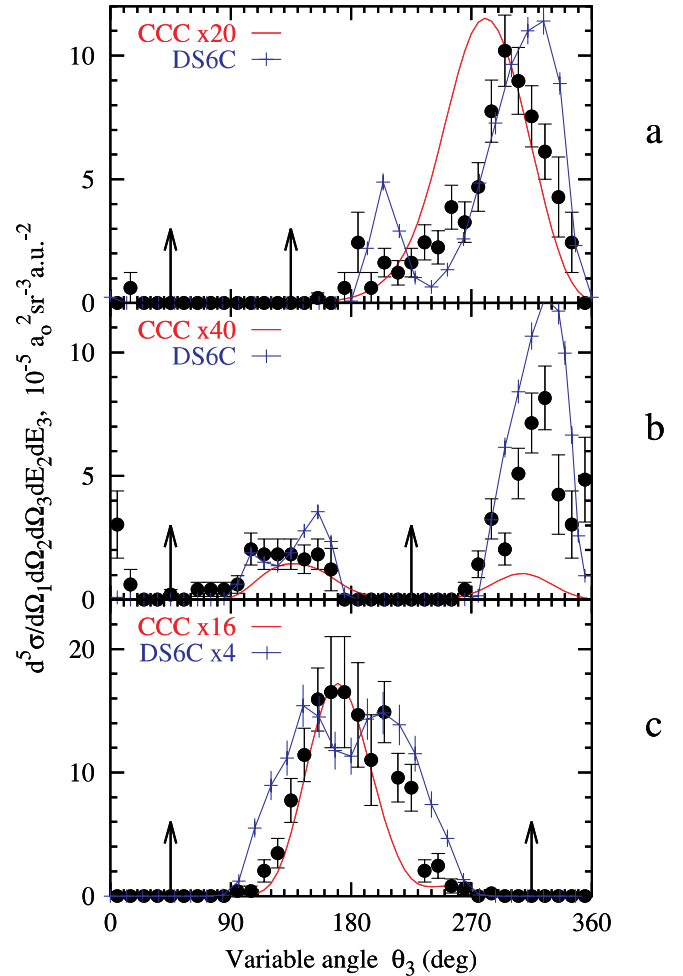


FIG. 3 (color online). FDCS for equal energy sharing $E_1 = E_2 = E_3 = 9 \pm 3$ eV and the coplanar geometry where the incoming projectile and all outgoing electrons move in a common plane. The cross sections are plotted as a function of θ_3 with respect to the incoming projectile forward direction. The emission angles of the other two electrons are fixed to $\theta_1 = 45^\circ$ and $\theta_2 = 135^\circ$ (a), 225° (b), and 315° (c). Directions of the fixed angle electrons are indicated by arrows. The full width at half maximum of the angular resolution is better than 15° .

variant of the 6C wave function (for details, see [26]). The DS6C model removes some of the deficiencies of the 6C model since, in contrast to 6C, it accounts for the screening of the two-body potential by the presence of further charged particles.

As an alternative model, we employ the first Born implementation of the CCC method [18], which describes the interaction between the two outgoing electrons exactly, whereas the interaction of each of the ejected electrons with the scattered projectile is approximated by the two-body Coulomb density of states, also known as the Gamow factor. The He ground state is represented by a 20 term Hylleraas expansion which recovers 99.98% of the correlation energy.

Results of both calculations are presented in Fig. 3 along with the experimental data. In Fig. 3(a), the CCC theory predicts only broad peak pointing almost exactly in the direction minimizing the Coulomb repulsion $\theta_3 = 270^\circ$. Conversely, the DS6C calculation shows two maxima. The larger one is situated near the position where the experiment shows its main peak. A smaller peak coincides with a long shoulder towards smaller emission angles seen in the experiment. One should note that the main peak is not located around $\theta_3 = 270^\circ$, which is the preferred direction for the third outgoing electron according to the Coulomb repulsion in this geometry. Rather, it is rotated slightly into the forward, incident beam direction (0° or, equivalently, 360°). The explanation of this effect is the memory of the direction of the impinging projectile which breaks the symmetry of the final state. This can be seen explicitly when the different spin-resolved components of the cross section are analyzed [26].

For the back-to-back configuration [Fig. 3(b)], the angular distance of e_3 relative to the nearest fixed angle electron cannot be larger than 90° , and, therefore, Coulomb repulsion strongly restricts the accessible angular range of θ_3 . Both calculations show peak position and width, agreeing with the experiment, but the relative height of the two peaks is better reproduced by the DS6C calculation, which shows a split structure in the left peak.

In Fig. 3(c), two of the emission angles are fixed symmetrically with respect to the projectile beam direction, and, therefore, the cross section, as a function of θ_3 , must be symmetric also with respect to $\theta_3 = 0^\circ$ and 180° . The CCC theory agrees well with the experiment concerning the shape, whereas the DS6C calculation displays a double-peak structure which is not clearly discernible in the experiment due to large error bars. On the other hand, for the geometries shown, the absolute size of the CCC calculation is wrong by 1–2 orders of magnitude. This is not surprising, considering the crude approximations (the Gamow factor and the first Born treatment) involved in this model. The absolute magnitude of the cross section is much better reproduced by the DS6C calculation. Only in Fig. 3(c) is there a considerable deviation from experiment.

In conclusion, we have investigated, both experimentally and theoretically, the $(e, 3e)$ reaction on He at low excess energy. The inspection of the global emission characteristics of the three outgoing electrons reveals their strongly correlated motion in the final state. Besides the equilateral triangle configuration predicted by threshold theory [20] and resulting in emission with 120° relative angles, the back-to-back configuration of two electrons with the third one being emitted perpendicular to the others is also observed. In a recent classical calculation [27], this configuration was predicted to dominate the three-electron escape even below 1 eV excess energy. Choosing equal energy sharing, an ideal three-electron continuum state is realized where the electrons are indistinguishable. The

shape of the resulting FDCS in coplanar geometry is dominated by the strong Coulomb repulsion in the final state. The observed emission pattern is predicted by a CCC calculation which accounts for the Coulomb interaction of the two ejected electrons in full, whereas the interaction of these with the third electron in the final state is approximated by a phenomenological Gamow factor. On the other hand, the absolute magnitude of the cross sections obtained by this rather crude approximation is wrong by more than 1 order of magnitude. A more sophisticated treatment of the full four-body Coulomb problem within the DS6C method shows better agreement concerning both the relative and the absolute peak heights. It also exhibits a richer structure of the cross section with distinct peaks, which are not entirely seen in the experiment. Since this model still exhibits deviations in the absolute scale up to a factor of 4 with respect to experiment, it is clear that the presently existing theoretical models are severely challenged by the experiment, and major improvements in theory are needed.

The Heidelberg team thanks R. Moshhammer for fruitful discussions. A. S. K. thanks MPI-Heidelberg for hospitality.

-
- [1] C.W. McCurdy, M. Baertschy, and T.N. Rescigno, *J. Phys. B* **37**, R137 (2004).
 - [2] J.S. Briggs and V. Schmidt, *J. Phys. B* **33**, R1 (2000).
 - [3] L. Avaldi and A. Huetz, *J. Phys. B* **38**, S861 (2005).
 - [4] D.H. Madison *et al.*, *Phys. Rev. Lett.* **91**, 253201 (2003).
 - [5] R. Wehlitz *et al.*, *Phys. Rev. A* **61**, 030704 (2000).
 - [6] T. Weber *et al.*, *Nature (London)* **431**, 437 (2004).
 - [7] M. Gisselbrecht *et al.*, *Phys. Rev. Lett.* **96**, 153002 (2006).
 - [8] W. Vanroose *et al.*, *Science* **310**, 1787 (2005).
 - [9] M. Walter, A. V. Meremianin, and J.S. Briggs, *J. Phys. B* **36**, 4561 (2003).
 - [10] M. Walter, A. Meremianin, and J.S. Briggs, *Phys. Rev. Lett.* **90**, 233001 (2003).
 - [11] M. Schulz *et al.*, *Phys. Rev. A* **61**, 022703 (2000).
 - [12] D. Fischer *et al.*, *Phys. Rev. Lett.* **90**, 243201 (2003).
 - [13] M. Schulz *et al.*, *J. Phys. B* **38**, 1363 (2005).
 - [14] A. Dorn *et al.*, *Phys. Rev. Lett.* **86**, 3755 (2001).
 - [15] I. Taouil *et al.*, *Phys. Rev. Lett.* **81**, 4600 (1998).
 - [16] A. Lahmam-Bennani *et al.*, *Phys. Rev. A* **59**, 3548 (1999).
 - [17] J.R. Götze, M. Walter, and J.S. Briggs, *J. Phys. B* **38**, 1569 (2005).
 - [18] A.S. Kheifets *et al.*, *J. Phys. B* **32**, 5047 (1999).
 - [19] A.S. Kheifets, *Phys. Rev. A* **69**, 032712 (2004).
 - [20] H. Klar and W. Schlecht, *J. Phys. B* **9**, 1699 (1976).
 - [21] A.W. Malcherek and J.S. Briggs, *J. Phys. B* **30**, 4419 (1997).
 - [22] S. Denifl *et al.*, *J. Phys. B* **35**, 4685 (2002).
 - [23] M. Dürr *et al.*, *J. Phys. B* **39**, 4097 (2006).
 - [24] J. Ullrich *et al.*, *Rep. Prog. Phys.* **66**, 1463 (2003).
 - [25] I. Bray and D.V. Fursa, *Phys. Rev. Lett.* **76**, 2674 (1996).
 - [26] J.R. Götze, M. Walter, and J.S. Briggs, *J. Phys. B* **39**, 4365 (2006).
 - [27] A. Emmanouilidou and J.M. Rost, *J. Phys. B* **39**, 4037 (2006).